EXPERIMENTAL PROCEDURES

Animal measurements

All mice were maintained according to National Institutes of Health guidelines and all animal use protocols were approved by the Institutional Animal Care and Use Committee. Studies used C57BL/6 wild type (wt) male 4-month-old mice, maintained on a standard chow diet (5053 PicoLab diet, Ralston Purina Company, St. Louis, MO). Mice were sacrificed at 7:00 am for fed-mouse studies, or transferred to a new cage without food for 24 h from 7:00 am to 7:00 am, and sacrificed for fasted-mouse studies. For continuous delivery of βOHB (Sigma-Aldrich, St. Louis, MO), osmotic pumps (ALZET model 2001D; 8 μL/hr) were implanted intraperitoneally. Control mice were infused with sterile PBS. βOHB concentrations were determined with a βOHB detection kit (Stanbio Laboratory, Boerne, TX).

Calorie Restriction Protocol

Male C57BL6/J mice (The Jackson Laboratories, Bar Harbor, MI) were randomly assigned to two groups at 16 weeks of age mice, singly housed, and maintained on a NIH-31 diet either ad libitum (AL) or calorie restricted (CR) until sacrifice. CR animals were fed daily weighed amounts equivalent to 60% of AL intake. Body weight was recorded biweekly. Mice were housed in an environmentally controlled vivarium with

unlimited access to water and a controlled photoperiod (12 h light; 12 h dark).

Cell culture and plasmid construction

HEK293 cells were cultured in DMEM supplemented with 10% FCS. βOHB (R-3-hydroxybutyrate) was purchased from Sigma-Aldrich (St. Louis, MO). All expression constructs were generated by standard PCR-based cloning strategies, and all expression constructs were verified by DNA sequencing. For shRNA-mediated HDAC knockdown, a short 19-mer hairpin was cloned into pSicoRMS2 vector, a modified pSicoR (EF1alpha-mCherry-T2A-Puro) (*23*). The target sequences were as follows: human HDAC1 (target sequence CGTTCTTAACTTTGAACCAATA), human HDAC2 (target sequence CAGTCTCACCAATTTCAGAAA), human HDAC3 (target sequence GTACCTATTAGGGATGAGAT), human HDAC4 (target sequence GCAGCTCAAGAACAAGGAGAA), human HDAC5 (target sequence GCTAGAGAAAGTCATCGAGAT), human HDAC6 (target sequence GCACAGTCTTATGGATGGCTA), human HDAC7 (target sequence GCCAGCAAGATCCTCATTGT), human HDAC8 (target sequence CCGAATCCAACAAATCCTCAA).

Acid extraction of histones

Snap-frozen mouse tissues were ground and dissolved in lysis buffer (1xPBS with 0.5% Triton, 2 mM PMSF, 0.02% NaN_3, and 5 mM sodium butyrate). Lysates were mixed with vortex for 10 min at 4^{o}C, centrifuged at 500 g, for 10 min at 4^{o}C. Precipitates were washed twice in 1/2 volume of lysis buffer, resuspended in 0.2 N HCL and incubated with agitation for overnight at 4^{o}C. Histones in supernatant were collected after centrifugation at 500 g for 10 min. Tris-base was added into the histone fraction to neutralize before SDS-PAGE.

Immunoblotting

Antibodies used were anti-α-tubulin, anti-acetylated α-tubulin, anti-Flag M2 or rabbit polyclonal anti-Flag (Sigma-Aldrich), anti-HA (12CA5 and 3F10; Roche Diagnostics, Indianapolis, IN), anti-histone H3, anti-Acetylated histone H3K9, anti-Acetylated histone H3K14 (Millipore, Billerica, MA), anti-acetylated-lysine polyclonal antibody (Cell Signaling Technology, Danvers, MA), anti-Complex Va antibody (Invitrogen, Carlsbad, CA), anti-MnSOD and anti-c-myc (Santa Cruz Biotechnology, Santa Cruz, CA). FOXO3a antiserum was gift from Dr. Anne Brunet. Immunoblots were developed with enhanced chemiluminescence (Amersham Pharmacia Biosciences, Piscataway, NJ) or West SuperSignal reagent (Pierce, Rockford, IL). Protein carbonylation was

detected with Oxiselect protein carbonyl Immunoblot kit (Cell Biolab, San Diego, CA).

Microarray analysis

Kidney tissues were removed from mice (16 weeks old, standard diet; n=3 for 24h fasting and fed; n=4 for βOHB osmotic pump and n=3 for PBS control) and RNA was extracted in Trizol (Invitrogen, Carlsbad, CA), according to the manufacturer's instructions. Samples were prepared using Affymetrix WT cDNA Synthesis and Amplification Kits and WT Target Labeling and Control Reagents, according to the manufacturer's instructions. Labeled cDNA samples were hybridized, stained, and scanned to Affymetrix Mouse Gene 1.0 ST arrays, according to manufacturer's instructions. Raw intensities from the CEL files were analyzed using Affymetrix Power Tools (APT, version 1.10.1) with standard background correction to generate an RMA [robust multi-array average (*24*)] intensity on a log2 scale for each probe set, as well as various quality metrics and detection against background (DABG). Probe sets were filtered for "present" detection in two or more arrays, and interquartile intensity range >0.5. The filtered RMA intensities were then analyzed for differential expression using the *limma* algorithm, as implemented in R/Bioconductor, which uses linear modeling and empirical Bayes methods to generate P values and calculates FDR via the Benjamini-Hochberg method.

Quantitative real time PCR

Total RNA was extracted from mouse tissues with Trizol reagent (Invitrogen) and cDNA was synthesized using Superscript II Reverse Transcriptase (Invitrogen, Carlsbad, CA) according to manufactures protocol. Gene expression was analyzed with a Taqman qPCR method (7900fast, Applied Biosystems). All primers were purchased from Applied Biosystems. Relative expression was calculated with a DDCT method after normalization to GAPDH.

ChIP analysis

Protein-DNA complex were cross-linked with formaldehyde, sonicated and immunoprecipitated with antibody conjugated protein A/G agarose beads (Santa Cruz Biotechnology, Santa Cruz, CA) at 4^{o}C overnight. Antibodies used for ChIP were: normal mouse IgG (Santa Cruz Biotechnology), anti-histoneH3, anti-Acetyl-H3K9 (Millipore), anti-HDAC1 or anti-HDAC6 (Santa Cruz Biotechnology) antibody. The immunoprecipitated DNA was recovered with proteinase K and purified with phenol/chloroform precipitation. Precipitated DNA was analyzed with SYBR green Q-PCR. The primer sets used for H3K9 promoter binding assay were as follows:

hMT2 0.1K-F CGCCTTCAGGGAACTGAC; hMT2 0.1K-R

AGTCACTTGCGGCTCCAG; hMT2 1K-F TTCCAGAGGCAGACAATGAC; hMT2 1K-R ATAAACTGCGGGGACTCTTG; hMT2 2K-F CAGCATTCCCAGCAAAAGTA; hMT2 2K-R TCCTAGGCCATTCCACCTAC; hFOXO3 0.1K-F AGAAGAGCCGAAGACAGCAC; hFOXO3 0.1K-R GTGTGCGTGCGTTTGTTTAT; hFOXO3 1K-F GGGCACGGATCGTAGAATAA; hFOXO3 1K-R ACGTGGGCATTTTTGACTTT; hFOXO3 2K-F CAGTGAGTGTGTGCAGCTTG; hFOXO3 2K-R AAAGCCTCCTGTTTGTGCTT; hFOXO3 10K-F CATTGTTCACTTGGGGATCA; hFOXO3 10K-R CAGCCATCTTGACCCATTT; hFOXO3 down-F TGCACACAGAAGCCAGAAG; hFOXO3 down-R GCTCCCCACAGAGACGTAA. The primer sets used for HDAC1 and HDAC6 promoter binding assay were as follows: hMT2 1-F AGCCGCAAGTGACTCAGC; hMT2 1-R CTAGAAAGAGCCGGGACGAG; hMT2 2-F CGCCTTCAGGGAACTGAC; hMT2 2-R AGTCACTTGCGGCTCCAG; hFOXO3 1-F GGCTAGGAAAGGGGAGAAGA; hFOXO3 1-R GTGCGTGCGTTTGTTTATGT; hFOXO3 2-F AGAAGAGCCGAAGACAGCAC; hFOXO3 2-R GTGTGCGTGCGTTTGTTTAT.

In vitro HDAC activity assay

Recombinant Flag-tagged HDAC proteins were expressed in HEK293 after transient

transfection, purified with anti-Flag M2 agarose beads and eluted with Flag peptide. Deacetylase assays were performed in 100 μl of deacetylase buffer (4 mM, MgCl2, 0.2 mM dithiothreitol, 50 mM Tris–HCl, pH 8.5) containing 50 ng of HDAC and [^{3}H]-histone H4 peptide substrate with or without βOHB. The substrate was prepared by *in vitro* acetylation of a histone H4 N-terminal peptide (amino acids 1–25) with ^{3}H-labeled acetyl-CoA and recombinant PCAF (*12*). Deacetylation reactions were conducted at 37^{0}C under gentle agitation and stopped by adding 25 μl of stop solution (0.2 M HCl, 0.32 M acetic acid). Released acetate was extracted into 500 μl ethyl acetate by vortex for 15 s. After centrifugation at 14,000g for 5 min, 450 μl of the ethyl acetate fraction was mixed with 5 ml of scintillation fluid (Perkin Elmer), and the radioactivity was measured with a liquid scintillation counter (Beckman LS6000).

Fluorometric HDAC assay and α-tubulin deacetylation assay were conducted as described (*25*).

Measurement of oxidative Stress

Lipid peroxides were directly quantified using an ELISA assay that measures conversion of ferrous ions to ferric ions with Lipid hydroperoxidase Assay Kit (Cayman, Ann Arbor, MI). Protein carbonylation was detected with Oxyblot Protein Oxidation Detection kit (Millipore).

Acetyl-CoA measurement

For acyl-CoA measurements, acyl CoA esters were extracted from cell treated with βOHB or PBS, analyzed and purified based on previously published methods (*26*). The acyl CoAs were analyzed by flow injection analysis using positive electrospray ionization on Quattro micro, triple quadrupole mass spectrometer (Waters, Milford, MA) employing methanol/water (80:20, v:v) containing 30 mM ammonium hydroxide as the mobile phase. Spectra were acquired in the multichannel acquisition mode monitoring the neutral loss of 507 amu (phosphoadenosine diphosphate) and scanning from m/z 750- 1060. Heptadecanoyl CoA and 13C2 acetyl CoA were employed as internal standards for the long and short chain CoA esters, respectively. The endogenous CoAs were quantified using calibrators prepared by spiking cell homogenates with authentic CoAs (Sigma-Aldrich, St. Louis, MO) having saturated acyl chain lengths C_0-C_{18} and unsaturated species of $C_{16:1}$, $C_{18:2}$, $C_{18:1}$ and $C_{20:4}$. Corrections for the heavy isotope effects, mainly ^{13}C, to the adjacent m+2 spectral peaks in a particular chain length cluster were made empirically by referring to the observed spectra for the analytical standards.

Statistical Analyses

Results are given as the mean ± standard error. Unless otherwise specified, statistical analyses represent a non-parametric Students t-test comparing an experimental condition to the relevant control condition. Null hypotheses were rejected at 0.05.

SUPPLEMENTARY FIGURES

Fig. S1. Histone hyperacetylation induced by increasing concentrations of βOHB *in vitro*. HEK293 cells were treated with the indicated concentrations of βOHB, and histones acid-extracted after 6 hours. Western blot as in Figure 1B.

Fig. S2. Histone hyperacetylation induced over various time points by βOHB *in vitro*. HEK293 cells were treated with the indicated concentrations of βOHB, and histones acid-extracted after 3, 6 and 12 hours. Western blot as in Figure 1B.

Fig. S3. HDAC1-associated activity is dependent on HDAC1 and βOHB does not inhibit HDAC6-mediated α-tubulin deacetylation

A. A mutation was introduced into HDAC1 (H141A) and the histone deacetylase activity associated with HDAC1 was assayed after transfection and immunoprecipitation as shown in Fig. 1D; Partially purified acetylated α-tubulin were mixed with HDAC6 for 2 h at 37^0C in the presence or absence of βOHB, butyrate or TSA. Acetylation was assessed by western blot with anti-Ac-α-tubulin antibody. Relative HDAC6 activity was normalized to the intensity of Ac-α-tubulin without drugs. Mean ± standard error.

Fig. S4. Acetyl-CoA level in βOHB treated HEK293T cells

HEK293T cells were treated with PBS or 10 mM βOHB for 8 h, and their acetyl-CoA level were measured. Mean ± standard error.

Fig. S5. βOHB **does not inhibit the histone acetyltransferase activity of p300 or PCAF.**

Recombinant p300 or PCAF were mixed with ^{14}C-labelled acetyl-CoA and purified histones in the presence or absence of βOHB. Acetylation of Histone H3 was analyzed with autoradiography. Representative HAT activity was shown.

Fig. S6. HDAC inhibition by acetoacetate and histone hyperacetylation in response to acetoacetate treatment in HEK293 cells

A. Recombinant HDACs were incubated with coumarin-labeled histone H3K12 peptide (*25*) with or without acetoacetate and enzymatic activity was measured; B. HEK293T cells were treated with indicated amount of acetoacetate for 8 h. Acetylation level of histone was analyzed with anti-AcH3$_{K9}$ or anti-AcH3$_{K14}$ antibody. Representative image and their relative acetylation after normalization with control histone acetylation are shown.

Fig S7. Relative roles of βOHB and acetoacetate in histone hyperacetylation in response to βOHB treatment.

A. HEK293 cells were transfected with siRNAs for βOHB dehydrogenases (BDH1, 2) and treated with βOHB at different concentrations (0-30 mM). Cells were harvested and the level of histone $H3_{K14}$ acetylation was assessed by western blotting. Depletion of BDH1/2 expression was confirmed by western blotting; B. Quantification of western blot shown in panel A.

Fig. S8. βOHB induces histone hyperacetylation *in vivo*. Fasting, calorie restriction, or delivery of exogenous βOHB via osmotic pump induce histone hyperacetylation in mouse kidney. Original images for data presented in Figs. 2C and 2D.

Fig S9. Tissue profile of histone acetylation in mice fasted for 24 hours vs. fed.

Histones were purified from various tissues of mice either fasted for 24 hours or fed normally. Acetylation of histones was assessed by slot blot using specific antisera for acetylated histone $H3_{K9}$, $H3_{K14}$, $H3_{K27}$, $H3_{K36}$ and H4. Stars indicate significant results ($p<0.05$).

Fig S10. Quantitative real-time PCR in mouse kidney.

FOXO3a network genes, which were identified in our microarray analysis as upregulated were confirmed by quantitative real-time PCR of mRNA isolated from βOHB-treated mice (24 h). Relative expression was normalized to mRNA levels isolated from mice implanted with a pump delivering PBS. All samples were normalize to GAPDH mRNA levels (n=3). Mean ± standard error, *p<0.05, **p<0.001.

Fig. S11. shRNA knockdown of HDAC expression. shRNA-expressing constructs were generated using unique sequence for HDAC1-8. They were transfected in HEK293 cells, and the relative expression of the cognate HDAC was assessed by western analysis. A representative western blot is shown (n=3). Loading controls for each blot are shown using an anti-α tubulin specific antiserum.

Fig. S12. Chromatin immunoprecipitation analysis of FOXO3a promoter in HEK293 cells treated with βOHB

ChIP of the FOXO3a promoter from HEK293 cells treated with PBS or βOHB (10 mM) with control IgG or anti-HDAC1 antisera. Relative promoter binding of each HDAC normalized to input GAPDH (n=3). Mean ± standard error.

Fig. S13. Western blots of oxidative stress proteins after βOHB treatment.

Amounts of catalase, MnSOD or FOXO3A measured by protein immunoblotting in kidney tissue from 16-week-old mice implanted with an osmotic pump delivering PBS or βOHB. Original images for data presented in Fig. 4A.

Fig. S14. RNA expression of Catalase and Mn-SOD

Expression levels of Catalase and Mn-SOD mRNA were analyzed by Q-PCR in kidney tissue from 16-week-old mice treated with PBS or βOHB (n=3)(same conditions as Fig. 2) Mean ± standard error, *$p<0.05$.

Fig. S15. Hydroxynonenal (HNE) staining of kidney tissues isolated from mice treated with PBS or βOHB and challenged with paraquat. Kidney obtained from the same mice as in Figure 4C, D are stained with anti-4-HNE antibody and quantified. Three random pictures per section (three sections per animal) were analyzed with Image J software (NIH). Images with an intensity above a predetermined threshold level was quantified by measurement of the number of pixels per image in areas that are immunoreactive for HNE. Total immunoreactivity was calculated as percent area density defined as the number of pixels (positively stained areas) divided by the total number of pixels (sum of positively and negatively stained area) in the imaged field.

Shimazu *et al*, Supplementary Figure 1

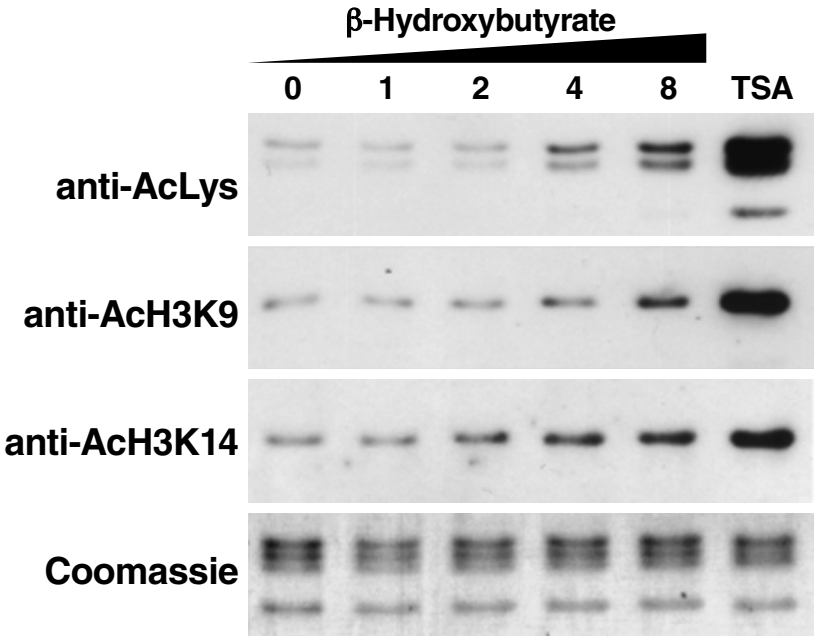

Shimazu *et al*, Supplementary Figure 2

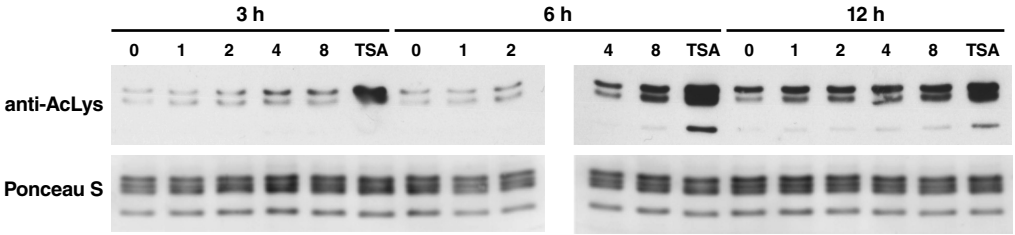

Shimazu *et al*, Supplementary Figure 3

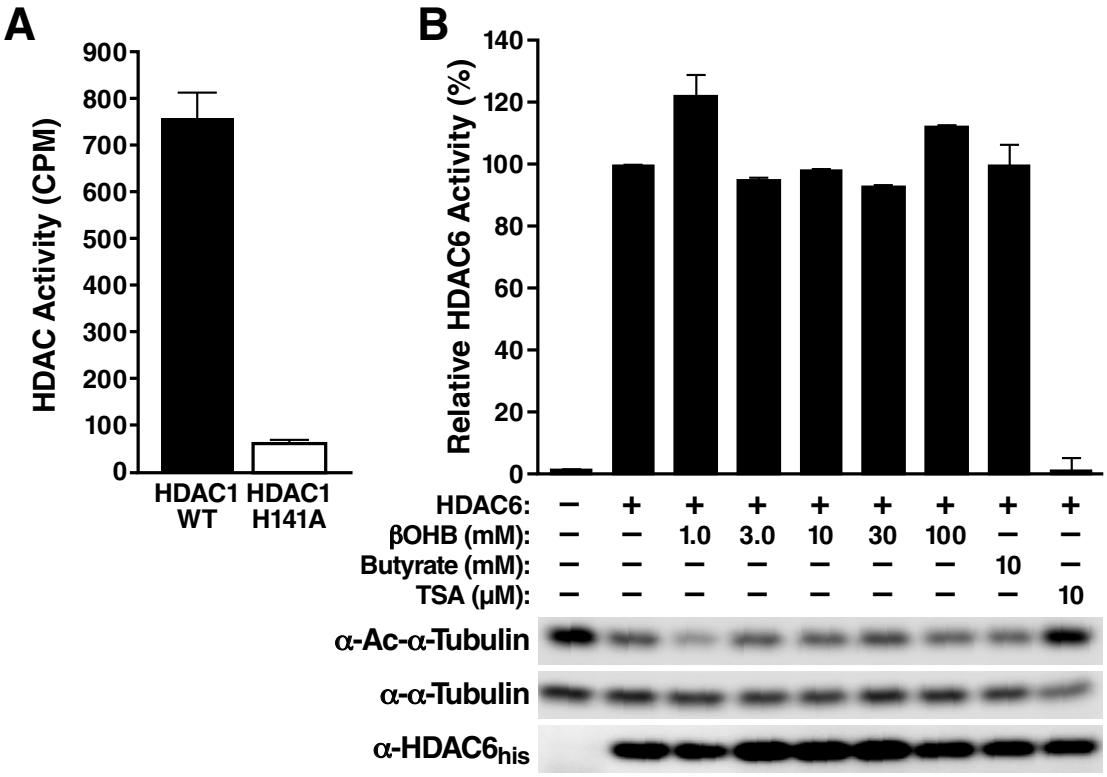

Shimazu *et al*, Supplementary Figure 4

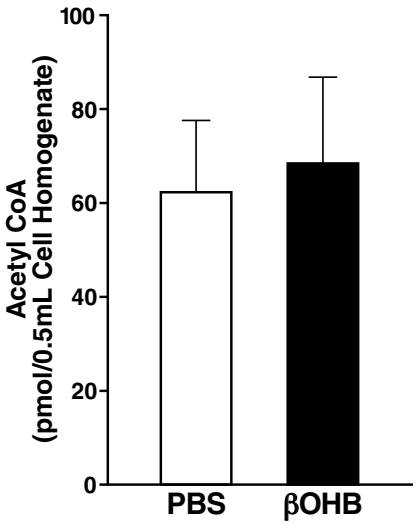

Shimazu *et al*, Supplementary Figure 5

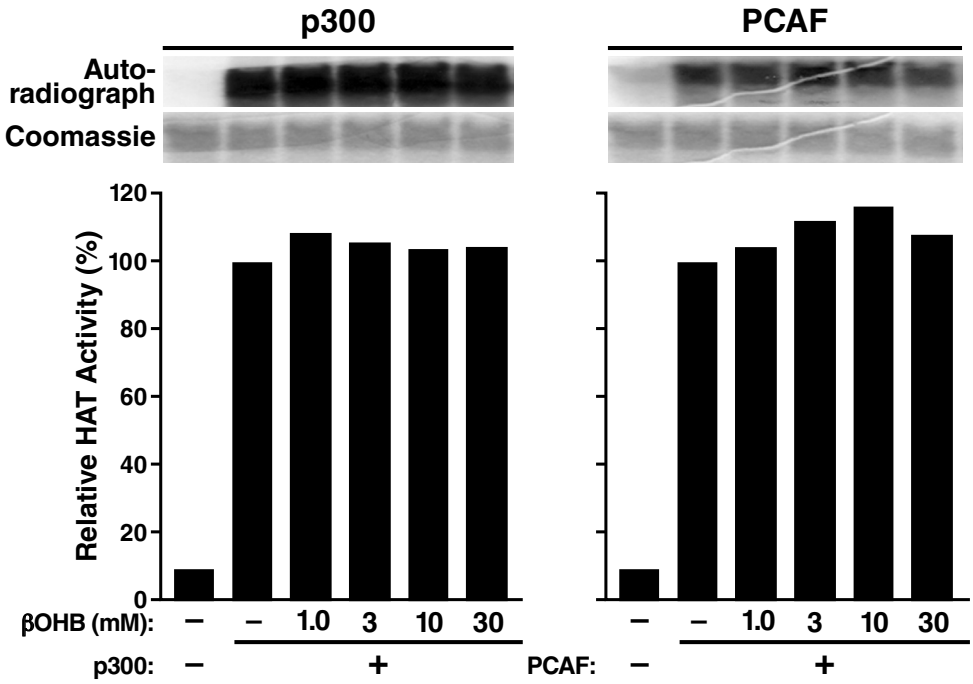

Shimazu *et al*, Supplementary Figure 6

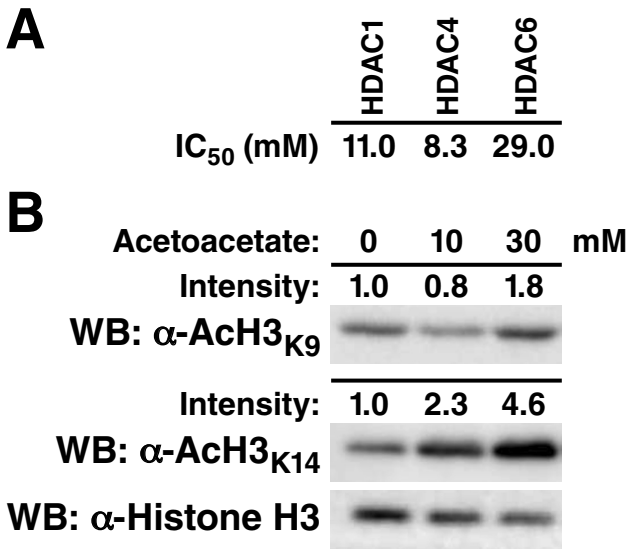

Shimazu *et al*, Supplementary Figure 7

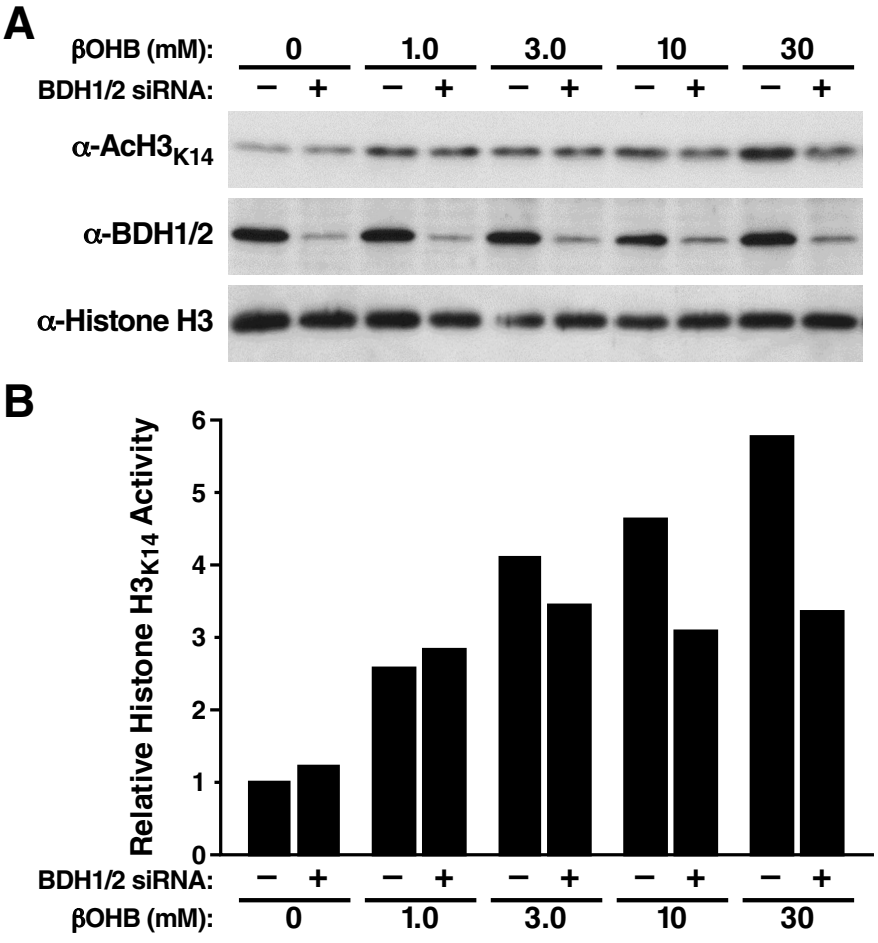

Shimazu *et al*, Supplementary Figure 8

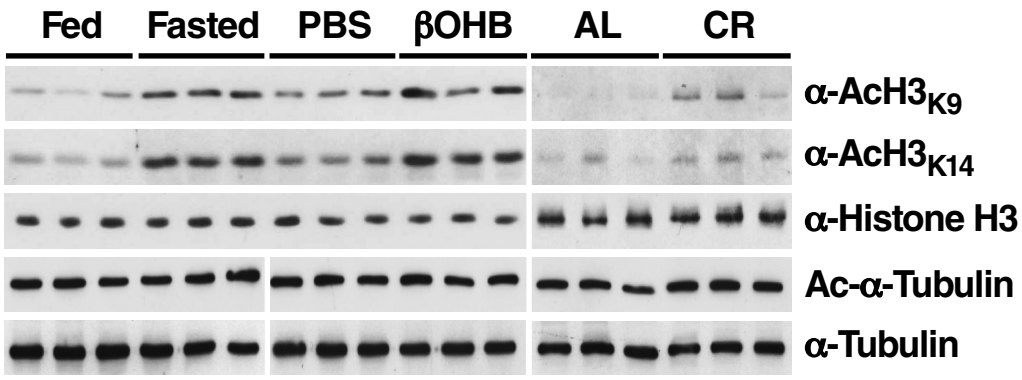

Shimazu *et al*, Supplementary Figure 9

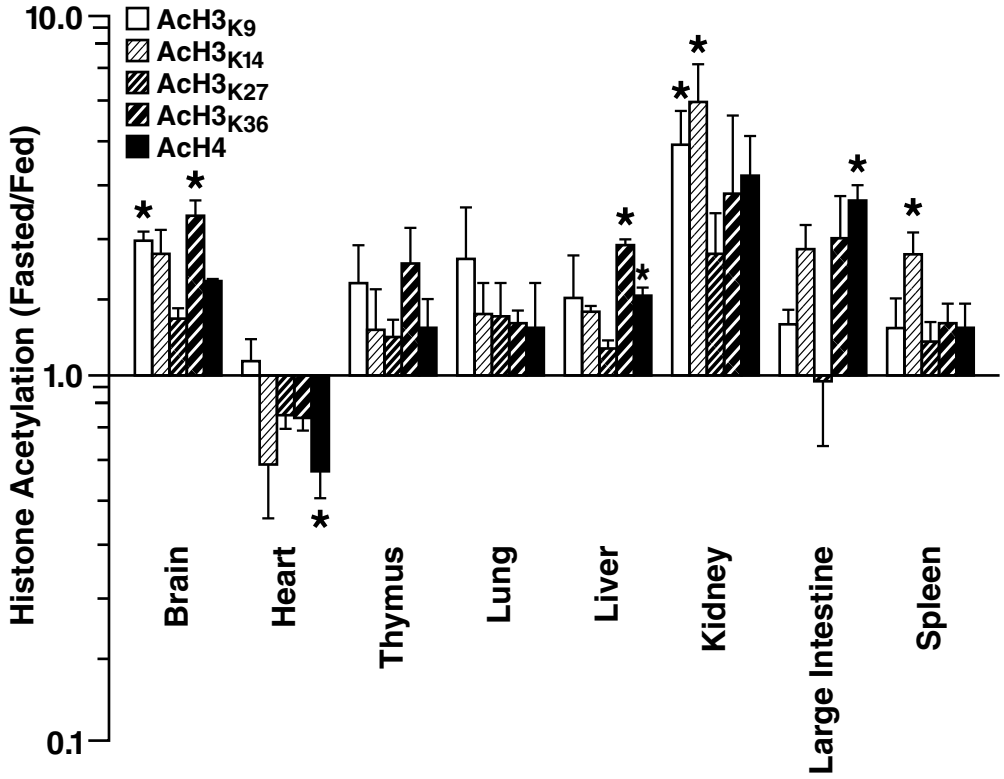

Shimazu *et al*, Supplementary Figure 10

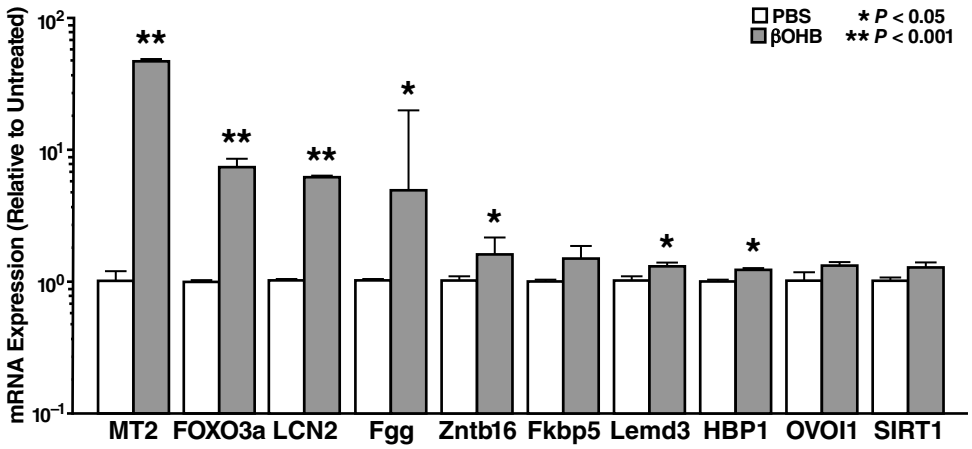

Shimazu *et al*, Supplementary Figure 11

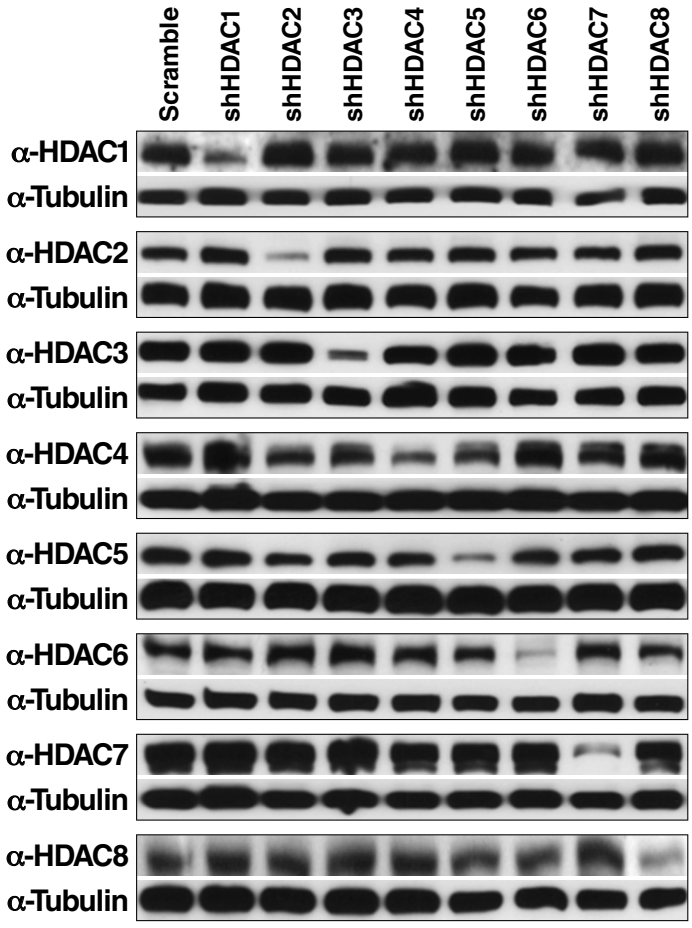

Shimazu *et al*, Supplementary Figure 12

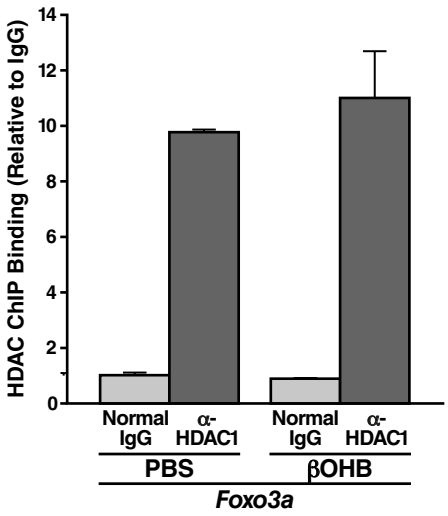

Shimazu *et al*, Supplememntary Figure 13

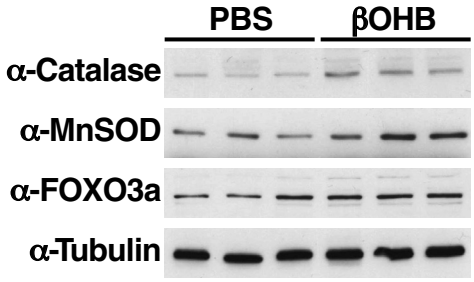

Shimazu *et al*, Supplementary Figure 14

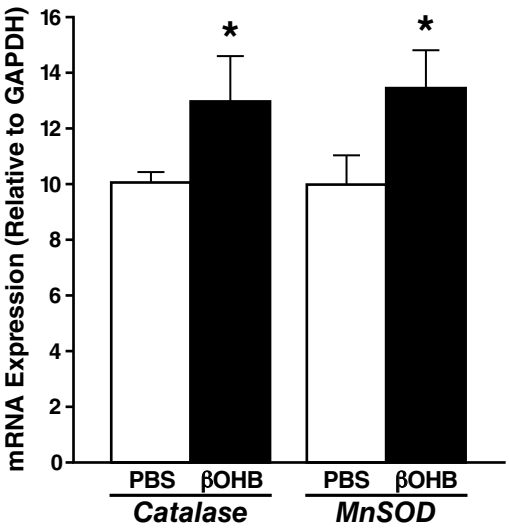

Shimazu *et al*, Supplementary Figure 15

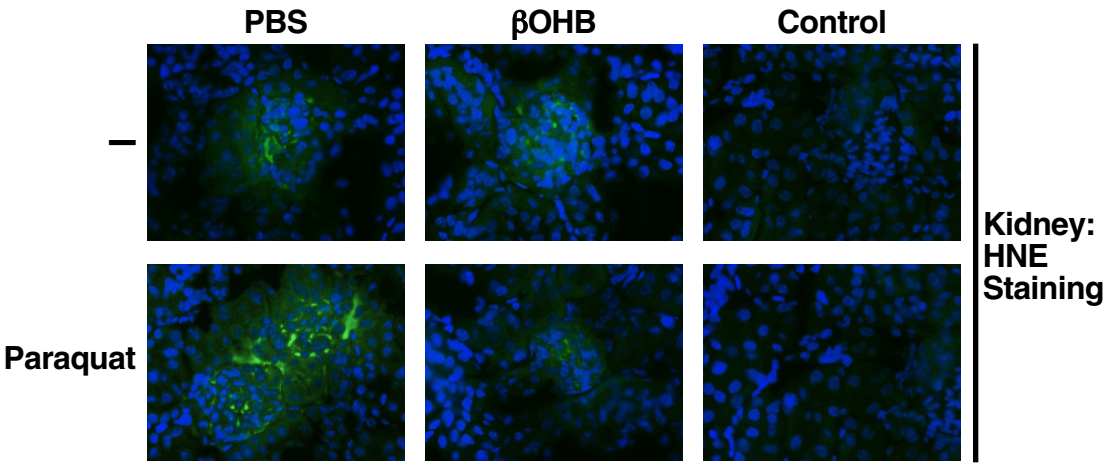

SUPPLEMENTARY TABLES

Table S1. Gene expression microarray data for kidney tissue from fed versus 24h-fasted mice (16 weeks old, standard diet; n=3 for 24h fasting and fed conditions).

Table S2. Gene expression microarray data for kidney tissue from mice implanted with osmotic pump delivering βOHB versus PBS control (16 weeks old, standard diet; n=4 for βOHB osmotic pump and n=3 for PBS control).

Table S3. Overlap of gene expression changes induced by βOHB and fasting. The top five genes (via *limma* P value) upregulated in kidney by βOHB osmotic pump are shown, along with their expression change in fasting.

Affymetrix TC	*Gene symbol*	*Gene description*	*BOHB/PBS Log2 Ratio*	*BOHB/PBS P value*	*Fasted/Fed Log2 Ratio*	*Fasted/Fed P value*
10492735	Fgg	fibrinogen gamma chain	2.1	0.0063	1.21	0.0002
10481627	Lcn2	lipocalin 2	1.9	0.0104	ns	ns
10593225	Zbtb16	zinc finger and BTB domain containing 16	1.17	0.0173	1.54	0.001
10449452	Fkbp5	FK506 binding protein 5	0.99	0.02	0.7	0.0154
10574023	Mt2	metallothionein 2	1.4	0.0218	0.74	0.0086

References and Notes

1. A. G. Ladurner, Rheostat control of gene expression by metabolites. *Mol. Cell* **24**, 1 (2006). doi:10.1016/j.molcel.2006.09.002 Medline

2. K. E. Wellen *et al*., ATP-citrate lyase links cellular metabolism to histone acetylation. *Science* **324**, 1076 (2009). doi:10.1126/science.1164097 Medline

3. H. Takahashi, J. M. McCaffery, R. A. Irizarry, J. D. Boeke, Nucleocytosolic acetyl-coenzyme a synthetase is required for histone acetylation and global transcription. *Mol. Cell* **23**, 207 (2006). doi:10.1016/j.molcel.2006.05.040 Medline

4. S. Imai, C. M. Armstrong, M. Kaeberlein, L. Guarente, Transcriptional silencing and longevity protein Sir2 is an NAD-dependent histone deacetylase. *Nature* **403**, 795 (2000). doi:10.1038/35001622 Medline

5. E. P. Candido, R. Reeves, J. R. Davie, Sodium butyrate inhibits histone deacetylation in cultured cells. *Cell* **14**, 105 (1978). doi:10.1016/0092-8674(78)90305-7 Medline

6. G. F. Cahill Jr., Fuel metabolism in starvation. *Annu. Rev. Nutr.* **26**, 1 (2006). doi:10.1146/annurev.nutr.26.061505.111258 Medline

7. G. F. Cahill Jr. *et al*., Hormone-fuel interrelationships during fasting. *J. Clin. Invest.* **45**, 1751 (1966). doi:10.1172/JCI105481 Medline

8. A. M. Robinson, D. H. Williamson, Physiological roles of ketone bodies as substrates and signals in mammalian tissues. *Physiol. Rev.* **60**, 143 (1980). Medline

9. L. Laffel, Ketone bodies: A review of physiology, pathophysiology and application of monitoring to diabetes. *Diabetes Metab. Res. Rev.* **15**, 412 (1999). doi:10.1002/(SICI)1520-7560(199911/12)15:6<412::AID-DMRR72>3.0.CO;2-8 Medline

10. J. H. Koeslag, T. D. Noakes, A. W. Sloan, Post-exercise ketosis. *J. Physiol.* **301**, 79 (1980). Medline

11. B. J. North, B. Schwer, N. Ahuja, B. Marshall, E. Verdin, Preparation of enzymatically active recombinant class III protein deacetylases. *Methods* **36**, 338 (2005). doi:10.1016/j.ymeth.2005.03.004 Medline

12. O. E. Owen *et al*., Rapid intravenous sodium acetoacetate infusion in man. Metabolic and kinetic responses. *J. Clin. Invest.* **52**, 2606 (1973). doi:10.1172/JCI107453 Medline

13. T. Agalioti *et al*., Ordered recruitment of chromatin modifying and general transcription factors to the IFN-beta promoter. *Cell* **103**, 667 (2000). doi:10.1016/S0092-8674(00)00169-0 Medline

14. C. Van Lint, S. Emiliani, E. Verdin, The expression of a small fraction of cellular genes is changed in response to histone hyperacetylation. *Gene Expr.* **5**, 245 (1996). Medline

15. G. J. Kops *et al*., Forkhead transcription factor FOXO3a protects quiescent cells from oxidative stress. *Nature* **419**, 316 (2002). doi:10.1038/nature01036 Medline

16. K. Kawai *et al*., Antioxidant and antiapoptotic function of metallothioneins in HL-60 cells challenged with copper nitrilotriacetate. *Chem. Res. Toxicol.* **13**, 1275 (2000). doi:10.1021/tx000119l Medline

17. S. Nemoto, T. Finkel, Redox regulation of forkhead proteins through a p66shc-dependent signaling pathway. *Science* **295**, 2450 (2002). doi:10.1126/science.1069004 Medline

18. T. Nyström, Role of oxidative carbonylation in protein quality control and senescence. *EMBO J.* **24**, 1311 (2005). doi:10.1038/sj.emboj.7600599 Medline

19. H. Esterbauer, R. J. Schaur, H. Zollner, Chemistry and biochemistry of 4-hydroxynonenal, malonaldehyde and related aldehydes. *Free Radic. Biol. Med.* **11**, 81 (1991). doi:10.1016/0891-5849(91)90192-6 Medline

20. Y. Kim *et al*., Ketone bodies are protective against oxidative stress in neocortical neurons. *J. Neurochem.* **101**, 1316 (2007). doi:10.1111/j.1471-4159.2007.04483.x Medline

21. B. Rogina, S. L. Helfand, S. Frankel, Longevity regulation by Drosophila Rpd3 deacetylase and caloric restriction. *Science* **298**, 1745 (2002). doi:10.1126/science.1078986 Medline

22. H. L. Kang, S. Benzer, K. T. Min, Life extension in Drosophila by feeding a drug. *Proc. Natl. Acad. Sci. U.S.A.* **99**, 838 (2002). doi:10.1073/pnas.022631999 Medline

23. A. Ventura *et al*., Cre-lox-regulated conditional RNA interference from transgenes. *Proc. Natl. Acad. Sci. U.S.A.* **101**, 10380 (2004). doi:10.1073/pnas.0403954101 Medline

24. R. A. Irizarry *et al*., Summaries of Affymetrix GeneChip probe level data. *Nucleic Acids Res.* **31**, e15 (2003). doi:10.1093/nar/gng015 Medline

25. M. P. Bhuiyan *et al*., Chlamydocin analogs bearing carbonyl group as possible ligand toward zinc atom in histone deacetylases. *Bioorg. Med. Chem.* **14**, 3438 (2006). doi:10.1016/j.bmc.2005.12.063 Medline

26. P. E. Minkler, J. Kerner, S. T. Ingalls, C. L. Hoppel, Novel isolation procedure for short-, medium-, and long-chain acyl-coenzyme A esters from tissue. *Anal. Biochem.* **376**, 275 (2008). doi:10.1016/j.ab.2008.02.022 Medline